

Accepted Manuscript

Research paper

Antimicrobial selectivity of ruthenium, rhodium, and iridium half sandwich complexes containing phenyl hydrazone Schiff base ligands towards *B. thuringiensis* and *P. aeruginosa* bacteria

Agreedha Lapasam, Lincoln Dkhar, Nidhi Joshi, Krishna Mohan Poluri, Mohan Rao Kollipara

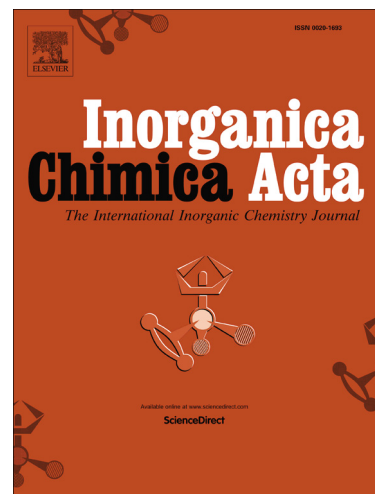
PII: S0020-1693(18)30733-3
DOI: <https://doi.org/10.1016/j.ica.2018.09.067>
Reference: ICA 18525

To appear in: *Inorganica Chimica Acta*

Received Date: 11 May 2018
Revised Date: 10 August 2018
Accepted Date: 20 September 2018

Please cite this article as: A. Lapasam, L. Dkhar, N. Joshi, K.M. Poluri, M. Rao Kollipara, Antimicrobial selectivity of ruthenium, rhodium, and iridium half sandwich complexes containing phenyl hydrazone Schiff base ligands towards *B. thuringiensis* and *P. aeruginosa* bacteria, *Inorganica Chimica Acta* (2018), doi: <https://doi.org/10.1016/j.ica.2018.09.067>

This is a PDF file of an unedited manuscript that has been accepted for publication. As a service to our customers we are providing this early version of the manuscript. The manuscript will undergo copyediting, typesetting, and review of the resulting proof before it is published in its final form. Please note that during the production process errors may be discovered which could affect the content, and all legal disclaimers that apply to the journal pertain.



Antimicrobial selectivity of ruthenium, rhodium, and iridium half sandwich complexes containing phenyl hydrazone Schiff base ligands towards *B. thuringiensis* and *P. aeruginosa* bacteria

Agreeda Lapasam^a, Lincoln Dkhar^a, Nidhi Joshi^b, Krishna Mohan Poluri^b,
Mohan Rao Kollipara^{a*}

^a*Centre for Advanced Studies in Chemistry, North-Eastern Hill University, Shillong-793 022, India.*

^b*Department of Biotechnology and Center for Nanotechnology, Indian Institute of Technology Roorkee, Roorkee-247667, Uttarakhand, India.*

E-mail: mohanrao59@gmail.com; kmrao@nehu.ac.in

Abstract

A series of new hydrazone mononuclear complexes of the type [(arene)MLCl]PF₆ (M = Ru, Rh, Ir) have been synthesized in this study. All these complexes were fully characterized with the help of FT-IR, UV-Vis, mass and NMR spectroscopy. The molecular structures of representative complexes (**1**, **2**, **7** and **8**) were established by single crystal X-ray diffraction study. The molecular structures of the complexes revealed typical piano stool geometry around the metal center in which the ligand acts as NN' donor chelating ligand. In the case of complexes (**1-3**), the ligand coordinates to the metal by using both the pyridine nitrogen atoms forming a six membered metallocycle whereas in complexes (**4-9**) one hydrazone nitrogen atom and one pyridine nitrogen atom coordinates to the metal ion forming a five membered metallocycle. These compounds were evaluated for their *in vitro* antibacterial activity by agar well diffusion method against two Gram-negative bacteria *Escherichia coli*, *Pseudomonas aeruginosa*, and two Gram-positive bacteria *Staphylococcus aureus*, *Bacillus thuriangiensis*. Results show that all the complexes inhibit the growth of bacteria.

Keywords: ruthenium, rhodium, iridium, hydrazone, antibacterial.

Introduction

Antimicrobials are one of the most significant weapons in fighting bacterial infections [1-2]. Antibacterial substances therefore are of great importance and necessity in treating infectious diseases caused by pathogenic bacteria [3-8]. However, the wide use of antibiotics caused pathogenic bacteria to grow increasingly resistant to commercially available antimicrobial agents, resulting in poor treatment efficacy and significant economic losses [9-11]. The increasing cases of microbial resistance pose a major concern to the scientific community and have become a threat for human life worldwide [12]. To overcome these problems, the development of new and safe antimicrobial agents with better effectiveness is required day by day. Therefore, the search for antimicrobials is a never-ending task. Now a day a number of hydrazone derivatives have been developed and evaluated for their antibacterial and antifungal activity [13]. Hydrazone derivatives also draw considerable attention due to their extensive applications in pharmaceutical and biological activities like anticancer [14], anti-inflammatory [15], antimalarial [16], antitubercular [17] activities. In previous studies, metallo elements such as, copper, cobalt, nickel, zinc and ruthenium, have been investigated because of their small size, comparatively high nuclear charge and consequently great ability to form coordination compounds [18-21]. But among the transition metal complexes, ruthenium-based complexes have been widely studied and displayed significant biological activity. This can be due to their ability to strongly bind nucleic acids and proteins, ligand exchange kinetics similar to those of their platinum counterparts, the prevalence of two main oxidation states (II and III) and the iron-mimicking property when bound to biological molecules [22-28]. In addition, both the commonly accessible oxidation states of ruthenium are octahedral and relatively inert and moreover the synthetic chemistry is very well established [27]. Over the last decade their therapeutic potential as anticancer and antimicrobial

agents have been demonstrated that may have advantages, such as minimal side effects and immunity to drug resistance [29-32].

Nevertheless, Cp*Rh and Cp*Ir complexes have also been considered as alternatives to ruthenium based drugs mainly because of their water solubility and inert facial co-ligand Cp* which allows half-sandwich complexes to be easily tailored for catalytic or biological applications. This has led to a growing interest in the chemistry of pentamethylcyclopentadienyl complexes of the type $[\text{Cp}^*\text{M}(\text{L})\text{Cl}]^{2+}$ (M = Rh/Ir, L a chelating ligand). These complexes have also been employed as catalysts for various organic reactions namely C-H activation, oxidation of alcohols, reduction of ketones and water oxidation. Rhodium(III) and iridium(III) complexes with nitrogen containing ligands have also been used as antibacterial as well as antitumor agents [33].

In our present work we report the synthesis of ruthenium, rhodium and iridium half-sandwich hydrazone complexes and their antibacterial activity have also been studied. Ligands used in this study are shown in Chart-1.

2. Experimental Section

2.1. *Physical methods and materials*

The reagents were of commercial quality and used without further purification. Di(2-pyridyl) ketone, α -phellandrene, pentamethylcyclopentadiene, 2- benzoyl pyridine and phenyl hydrazine were purchased from Sigma-Aldrich. 2,4 Di-Nitro phenyl hydrazine was obtained from Alfa Aesar. The syntheses of all the metal complexes were performed without using any inert atmosphere. All solvents used for syntheses were dried and distilled prior to use according to standard procedures [34]. Starting compounds $[(p\text{-cymene})\text{RuCl}_2]_2$ and $[\text{Cp}^*\text{MCl}_2]_2$ (M = Rh/Ir) were prepared according to literature methods [35-36]. Infrared (IR) spectra (400-4000

cm⁻¹) were recorded on a Perkin-Elmer 983 spectrophotometer with compounds being dispersed as KBr discs. ¹H NMR spectra were recorded on a Bruker Avance II 400 MHz instrument using CDCl₃ and DMSO-d₆ as solvents chemical shifts were referenced to TMS. Mass spectra were obtained from Waters ZQ 4000 mass spectrometer by ESI method using acetonitrile as solvent. Absorption spectra were recorded on a Perkin-Elmer Lambda 25 UV/Vis spectrophotometer in the range of 200-600 nm at room temperature in acetonitrile. Elemental analyses of the complexes were performed on a Perkin-Elmer 2400 CHN/S analyzer.

2.2. Structure determination by X-ray crystallography

Crystals suitable for X-ray analyses for complexes (**1**, **2**, **7** and **8**) were obtained by slow diffusion of the solutions of the compounds in dichloromethane with a fourfold excess of hexane and allowing them to stand undisturbed for three days. The single crystals of complexes were attached to a glass fiber and placed into the Oxford Diffraction Xcalibur Eos Gemini diffractometer. Single crystal X-ray diffraction data for the complexes were collected on an Oxford Diffraction Xcalibur Eos Gemini diffractometer using graphite monochromated Mo-K α radiation ($\lambda = 0.71073 \text{ \AA}$). The strategy for the data collection was evaluated using the CrysAlisPro CCD software. Crystal data were collected by standard “phi-omega scan” techniques and were scaled and reduced using CrysAlisPro RED software. The structures were solved by direct methods using SHELXS-97 and refined by full-matrix least squares with SHELXL-97 refining on F² [37-38]. The metal atoms in the complex were located from the E-maps and non-hydrogen atoms were refined anisotropically. The hydrogen atoms bound to the carbon were placed in geometrically constrained positions and refined with isotropic temperature factors, generally 1.2 U_{eq} of their parent atoms. The crystallographic and structure refinement parameters for the complexes are listed in Table 1 and selected bond lengths and bond angles are

presented in Table 2. Figures 1-3 were drawn with ORTEP3 program whereas Figures S14-S17 was drawn using MERCURY 3.6 program [39].

2.3. *In vitro* antimicrobial assay

The effect of synthesized complexes on the broad spectrum of bacterial strains was assayed by agar well diffusion method. In the present study, two-gram positive (*Staphylococcus aureus*; *Bacillus thuringiensis*) and two-gram negative (*Escherichia coli*, *Pseudomonas aeruginosa*) bacterial strains have been used. The agar nutrient broth media was prepared, sterilized at 121°C for 15 min. The chosen bacterial strains were inoculated in nutrient broth and incubated for overnight. Petriplates containing 30 ml of fresh Muller Hinton (MH) agar medium were seeded with 24 hour grown culture of bacterial strains. Wells of 5 mm diameter were cut and 100 µl of the each complex were added. The plates were then incubated at 37°C for 24 hours. The antibacterial activity was evaluated by measuring the diameter of the inhibition zone formed around the well. Each experiment was performed in triplicate. For well diffusion assay 1 mg mL⁻¹ concentration of complexes were used. Dimethylsulphoxide (DMSO) was used as a negative control and the antibiotic gentamycin was applied as positive control drug.

2.3. *Fluorescence studies on DNA interaction*

Salmon milt DNA (SM-DNA) was used for DNA binding experiments. SM-DNA was dissolved in 5 mM Tris-HCl and 50 mM NaCl buffer of pH 7.4. The concentration of DNA/nucleotide was evaluated by measuring UV-absorption at the wavelength of 260 nm. The fluorescence titration experiments of complexes were performed at a fixed concentration of ligand **L1**, complex **1** and complex **2** metal complexes (20µM) with increasing concentration of DNA (5-40 µM). The emission spectra of compounds were recorded at 390-600 nm by exciting ligand **L1**, complex **1** and complex **2** at 375 nm, 380 nm and 365 nm respectively. All

fluorescence titration experiments were recorded at room temperature and the samples were allowed to incubate for 15 min to attain thermodynamic equilibrium before spectral recording.

2.4. General procedure for preparation of ligands.

The ligands (**L1-L3**) were synthesized by modified literature methods [40-41] by mixing equimolar amounts of di(2-pyridyl)ketone or 2-benzoylpyridine with phenyl hydrazine in methanol and stirred for 30 minutes. To this solution three drops of acetic acid was added and the reaction mixture was kept under reflux for 6 h. After cooling to room temperature the resulting solids were filtered off, washed with ethanol and ether and dried in vacuum.

2.5. General procedure for synthesis of cationic complexes (**1-3**)

A mixture of starting metal precursor (0.1 mmol) and ligand di(2-pyridyl)ketone 2,4-dinitrophenylhydrazone (**L1**) (0.2 mmol) and 2.5 equivalents of NH_4PF_6 were dissolved in dry methanol (15 ml) and stirred at room temperature for 8 hours (Scheme-1). The solvent was evaporated to dryness. The residue was then dissolved in dichloromethane and filtered through a bed of celite to remove excess NH_4Cl . The filtrate was concentrated to 1 ml and on addition of excess hexane yellow solid precipitates out. The precipitate was further washed with diethyl ether and dried in vacuum.

2.5.1. [(*p*-cymene) RuL1Cl] PF_6 (**1**)

Yield: 87%; IR (KBr, cm^{-1}): 3313 $\nu_{(\text{N-H})}$, 3160 $\nu_{(\text{C-H})}$, 1614 $\nu_{(\text{C=N})}$, 1505, 1328 $\nu_{(\text{N-O})}$ 841 $\nu_{(\text{P-F})}$ (stretching) 558 $\nu_{(\text{P-F})}$ (bending); ^1H NMR (400 MHz) [$(\text{CD}_3)_2\text{SO}$] (ppm): 11.79 (s, 1H, NH), 9.31 (d, 2H, J = 8Hz), 7.97-8.14 (m, 4H), 7.64 (t, 1H, J = 8Hz), 7.58 (d, 2H, J = 8Hz), 7.45 (d, 2H, J = 12Hz), 6.14 (d, 2H, J = 4Hz), 5.93 (d, 2H, J = 4Hz), 2.92-2.99 (sept, 1H), 2.28 (s, 3H), 1.22 (d, 6H, J = 8Hz); ESI-MS (m/z): 635.06 $[\text{M-PF}_6]^+$; UV-Vis {Acetonitrile, λ_{max} , nm ($\epsilon/10^{-4} \text{ M}^{-1} \text{ cm}^{-1}$)

¹): 230 (5.65), 365 (4.69). Anal. Calc. for C₂₇H₂₆ClN₆O₄RuPF₆ (780.02): C, 41.57; H, 3.36; N, 10.77. Found: C, 41.68; H, 3.33; N, 10.91%.

2.5.2. [Cp*RhL1Cl]PF₆ (2)

Yield: 83%; IR (KBr, cm⁻¹): 3293 ν_(N-H), 3109 ν_(C-H), 1618 ν_(C=N), 1504, 1342 ν_(N-O), 843 ν_(P-F) (stretching) 558 ν_(P-F) (bending); ¹H NMR (400 MHz) [(CD₃)₂SO] (ppm) : 11.75 (s, 1H), 9.08 (d, 1H, J = 8Hz), 8.46 (t, 1H, J = 8Hz), 8.17-8.39 (m, 5H), 8.01 (t, 1H, J = 8Hz), 7.91 (t, 1H, J = 8Hz), 7.82 (t, 1H, J = 8Hz), 1.43 (s, 15H); ESI-MS (m/z): 637.01 [M-PF₆]⁺; UV-Vis {Acetonitrile, λ_{max}, nm (ε/10⁻⁴ M⁻¹ cm⁻¹): 265 (2.58), 365 (3.72). Anal. Calc. for C₂₇H₂₇ClN₆O₄RhPF₆ (782.86): C, 41.42; H, 3.48; N, 10.73. Found: C, 41.55; H, 3.50; N, 10.87%.

2.5.3. [Cp*IrL1Cl]PF₆ (3)

Yield: 76%; IR (KBr, cm⁻¹): 3295 ν_(N-H), 3115 ν_(C-H), 1617 ν_(C=N), 1503, 1331 ν_(N-O), 843 ν_(P-F) (stretching) 558 ν_(P-F) (bending); ¹H NMR: (400 MHz) [(CD₃)₂SO] (ppm): 11.75 (s, 1H), 9.05 (d, 1H, J = 4Hz), 8.79 (d, 1H, J = 8Hz), 8.43 (t, 1H, J = 8Hz), 8.16-8.38 (m, 5H), 7.97 (t, 1H, J = 8Hz), 7.89 (t, 1H, J = 8Hz), 7.78 (t, 1H, J = 8Hz), 1.39 (s, 15H); ESI-MS (m/z): 727.10 [M-PF₆]⁺; UV-Vis {Acetonitrile, λ_{max}, nm (ε/10⁻⁴ M⁻¹ cm⁻¹): 260 (2.20), 350 (2.97). Anal. Calc. for C₂₇H₂₇ClN₆O₄IrPF₆ (872.18): C, 37.18; H, 3.12; N, 9.64. Found: C, 37.29; H, 3.07; N, 9.77%.

2.6. General procedure for synthesis of cationic complexes (4-6)

A mixture of starting metal precursor (0.1 mmol) and ligand 2-benzoylpyridine 2,4-dinitrophenylhydrazone (**L2**) (0.2 mmol) were dissolved in dry methanol (15 ml) and stirred at room temperature for 8 hours (Scheme-2). A yellow colored compound precipitated out from the reaction mixture. The precipitate was filtered, washed with cold methanol and diethyl ether and dried in vacuum.

2.6.1. [(p-cymene)RuL2Cl]Cl (4)

Yield: 81%; 3306 $\nu_{(\text{N-H})}$, 3117 $\nu_{(\text{C-H})}$, 1621 $\nu_{(\text{C=N})}$, 1513, 1329 $\nu_{(\text{N-O})}$; $^1\text{H NMR}$ (400 MHz) $[(\text{CD}_3)_2\text{SO}]$ (ppm): 8.96 (d, 3H, $J = 4\text{Hz}$), 8.89 (s, 1H), 8.42 (d, 2H, $J = 12\text{Hz}$), 8.19 (d, 2H, $J = 8\text{Hz}$), 8.06 (t, 2H, $J = 8\text{Hz}$), 7.44 (d, 3H, $J = 8\text{Hz}$), 5.80 (d, 2H, $J = 8\text{Hz}$), 5.76 (d, 2H, $J = 8\text{Hz}$), 2.80 (sept, 1H), 2.06 (s, 3H), 1.16 (d, 6H, $J = 4\text{Hz}$); ESI-MS (m/z): 634.52 $[\text{M-Cl}]^+$; UV- Vis {Acetonitrile, λ_{max} , nm ($\epsilon/10^{-4} \text{M}^{-1} \text{cm}^{-1}$): 270 (2.94), 390 (2.53), 525 (1.28). Anal. Calc. for $\text{C}_{28}\text{H}_{27}\text{Cl}_2\text{N}_5\text{O}_4\text{Ru}^-$ (669.52): C, 50.23; H, 4.06; N, 10.46. Found: C, 50.38; H, 4.21; N, 10.54%.

2.6.2. $[\text{Cp}^*\text{Rh L2Cl}] \text{Cl}$ (**5**)

Yield: 76%; IR (KBr, cm^{-1}): 3303 $\nu_{(\text{N-H})}$, 3107 $\nu_{(\text{C-H})}$, 1621 $\nu_{(\text{C=N})}$, 1516, 1350 $\nu_{(\text{N-O})}$; $^1\text{H NMR}$ (400 MHz, CDCl_3) (ppm): 11.20 (s, 1H), 9.03 (d, 1H, $J = 4\text{Hz}$), 8.32 (d, 1H, $J = 8\text{Hz}$), 8.17 (d, 1H, $J = 12\text{Hz}$), 7.61-7.66 (m, 4H), 7.32-7.41 (m, 5H), 1.56 (s, 15H); ESI-MS (m/z): 636.15 $[\text{M-Cl}]^+$; UV- Vis {Acetonitrile, λ_{max} , nm ($\epsilon/10^{-4} \text{M}^{-1} \text{cm}^{-1}$): 265 (1.85), 375 (1.35).

2.6.3. $[\text{Cp}^*\text{Ir L2Cl}] \text{Cl}$ (**6**)

Yield: 89%; IR (KBr, cm^{-1}): 3305 $\nu_{(\text{N-H})}$, 3113 $\nu_{(\text{C-H})}$, 1623 $\nu_{(\text{C=N})}$, 1508, 1341 $\nu_{(\text{N-O})}$; $^1\text{H NMR}$ (400 MHz, CDCl_3) (ppm) : 11.41 (s, 1H), 9.46 (s, 1H), 9.10 (d, 1H, $J = 4 \text{ Hz}$), 8.33 (t, 1H, $J = 12\text{Hz}$), 8.26 (d, 1H, $J = 8\text{Hz}$), 7.84 (t, 2H, $J = 8\text{Hz}$), 7.65 (t, 2H, $J = 8\text{Hz}$), 7.50 (d, 2H, $J = 4\text{Hz}$), 7.44 (d, 1H, $J = 8\text{Hz}$), 7.41 (d, 1H, $J = 8\text{Hz}$); ESI-MS (m/z): 741.71 $[\text{M-Cl}]^+$; UV- Vis {Acetonitrile, λ_{max} , nm ($\epsilon/10^{-4} \text{M}^{-1} \text{cm}^{-1}$): 235 (2.47), 375 (1.08). Anal. Calc. for $\text{C}_{28}\text{H}_{28}\text{Cl}_2\text{IrN}_5\text{O}_4^-$ (689.04): C, 44.15; H, 3.71; N, 9.19. Found: C, 44.57; H, 3.68; N, 9.32%.

2.7. General procedure for synthesis of cationic complexes (**7-9**)

A mixture of starting metal precursor (0.1 mmol) and ligand 2 benzoyl pyridine phenyl hydrazine (**L3**) (0.2 mmol) and 2.5 equivalents of NH_4PF_6 were dissolved in dry methanol (15 ml) and stirred at room temperature for 8 hours (Scheme-3). The solvent was evaporated to dryness and the residue was dissolved in dichloromethane and filtered to remove excess NH_4Cl .

The filtrate was then concentrated to 1 ml and addition of excess hexane resulted in the precipitation of the compound. The precipitate was further washed with diethyl ether and dried in vacuum.

2.7.1. [(*p*-cymene)RuL3Cl]PF₆ (7)

Yield: 72%; IR (KBr, cm⁻¹): 3298 $\nu_{(N-H)}$, 3152 $\nu_{(C-H)}$, 1619 $\nu_{(C=N)}$, 844 $\nu_{(P-F)}$ (stretching) 560 $\nu_{(P-F)}$ (bending); ¹H NMR (400 MHz, CDCl₃) (ppm): 9.29 (d, 1H, J = 4Hz), 8.30 (s, 1H), 8.86 (t, 1H, J = 8Hz), 7.74 (t, 1H, J = 4Hz), 7.63 (t, 2H, J = 8Hz), 7.55 (d, 4H, J = 8Hz), 7.45 (t, 2H, J = 8Hz), 7.15-7.22 (m, 3H), 5.74 (d, 1H, J = 8Hz), 5.68 (d, 1H, J = 8Hz), 5.46 (d, 1H, J = 8Hz), 4.71 (d, 1H, J = 4Hz), 2.71-2.78 (sept, 1H), 2.04 (s, 6H), 1.16 (d, 3H, J = 4Hz), 1.08 (d, 3H, J = 8Hz), ESI-MS (m/z): 544.20 [M-PF₆]⁺; UV-Vis {Acetonitrile, λ_{max} , nm ($\epsilon/10^{-4}$ M⁻¹ cm⁻¹): 245 (2.49), 390 (1.25).

2.7.2. [Cp*RhL3Cl]PF₆ (8)

Yield: 64%; IR (KBr, cm⁻¹): 3295 $\nu_{(N-H)}$, 3114 $\nu_{(C-H)}$, 1621 $\nu_{(C=N)}$, 845 $\nu_{(P-F)}$ (stretching) 560 $\nu_{(P-F)}$ (bending); ¹H NMR (400 MHz, CDCl₃) (ppm): 8.72 (d, 1H, J=8Hz), 8.31 (s, 1H), 7.93 (t, 1H), 7.80 (d, 2H, J = 8Hz), 7.71 (t, 1H, J = 8Hz), 7.63 (t, 1H, J = 8Hz), 7.52 (d, 2H, J = 8Hz), 7.47 (d, 2H, J = 8Hz), 7.37 (t, 2H, J = 8Hz), 7.24 (d, 1H, J = 8Hz), 7.13 (t, 2H, J = 4Hz), 1.52 (s, 15H); ESI-MS (m/z): 546.23 [M-PF₆]⁺; UV-Vis {Acetonitrile, λ_{max} , nm ($\epsilon/10^{-4}$ M⁻¹ cm⁻¹): 260 (2.52), 355 (3.87). Anal. Calc. for C₂₈H₃₀ClN₃RhPF₆ (691.88): C, 48.61; H, 4.37; N, 6.07. Found: C, 48.73; H, 4.52; N, 6.19%.

2.7.3. [Cp*IrL3Cl]PF₆ (9)

Yield: 73%; IR (KBr, cm⁻¹): 3300 $\nu_{(N-H)}$, 3118 $\nu_{(C-H)}$, 1622 $\nu_{(C=N)}$, 841 $\nu_{(PF_6)}$ (stretching) 561 $\nu_{(PF_6)}$ (bending); ¹H NMR (400 MHz, CDCl₃) (ppm): 9.29 (s, 1H), 8.75 (d, 1H, J = 4Hz), 7.98

(t, 1H, J = 8Hz), 7.73-7.80 (m, 9H), 1.52 (s, 15H); ESI-MS (m/z): 636.15 [M-PF₆]⁺; UV- Vis {Acetonitrile, λ_{max} , nm ($\epsilon/10^{-4} \text{ M}^{-1} \text{ cm}^{-1}$)}: 245 (2.81), 265 (2.42), 320 (2.03), 420 (3.98).

3. RESULT AND DISCUSSION

3.1. Synthesis of complexes

The mononuclear complexes (1-9) were synthesized by the reaction of precursor complexes with the ligands L1-L3 in methanol as presented in schemes 1-3. Complexes **1-3** and **7-9** were isolated as cationic complexes with PF₆ as counter ion whereas complexes **4-6** were isolated as cationic complexes with chloride as counter ion. All these metal complexes were obtained in good yield and are non hygroscopic. The complexes were obtained as yellow solids and were found to be soluble in common organic solvents like dichloromethane, acetone and acetonitrile but insoluble in petroleum ether, hexane and diethyl ether. The synthesized complexes were characterized by various spectroscopic techniques and the molecular structures of some of the complexes were established by single crystal X-ray analysis.

3.2. Spectral studies of complexes (1-9)

The preliminary confirmation of the formation of complexes 1-9 can be justified to some extent from their IR spectra. Complexes (1-9) exhibit characteristic bands around 3300 cm⁻¹, 1619 cm⁻¹ which correspond to the stretching frequencies of N-H and C=N respectively. A strong band is also observed in the IR spectra of the complexes (1-6) in the region 1503–1516 cm⁻¹, which correspond to the asymmetric stretching vibration $\nu_{\text{N-O}}$ while the symmetric stretching vibration is observed in the region 1328–1350 cm⁻¹. These bands appear in the lower frequency regions compared to the free ligands L1-L3 where the $\nu_{\text{(N-H)}}$, $\nu_{\text{(C=N)}}$ are observed at 3400, 1638 cm⁻¹ respectively suggesting the coordination of the ligands to the metal centers. In

addition, these complexes show a characteristic stretching and bending frequencies for P-F counter anions around 844 cm^{-1} and 550 cm^{-1} respectively.

To reveal the coordination behavior of the ligands to metal in complexes the ^1H NMR analyses of the ligand and complexes were recorded in deuterated solvent at room temperature. The ^1H NMR spectra of complexes (**1-9**) display one singlet in the range 8.31-11.75 ppm for the NH proton which shift to the down field region with respect to the free ligand indicating the coordination of the ligand to the metal center. It may be mentioned that in few complexes the NH signal is not observed due to solvent interaction. The protons signals of the pyridine ring are observed as doublets in the downfield region around of 9.06-8.79 ppm indicating the coordination of the pyridyl nitrogen to the metal center which arises due to the donation of lone pairs of electron from the nitrogen atom to the metal center. In all the complexes the aromatic proton signals associated with the ligands are observed in the range 8.47–7.04 ppm. Complexes (1), (4) and (7) display a singlet and septet in the range 2.04-2.99 ppm corresponding to the methyl group and methine protons of the isopropyl group of the p-cymene ligand. The signal for the methyl protons of the isopropyl group is observed as one doublet in the range 1.07-1.21 ppm for complexes (1) and (4) and two doublets for complex (7) instead of one doublet as observed in the metal precursor. In addition, a singlet at 1.39-1.61 ppm is observed in complexes 2, 3, 5, 6, 8 and 9 corresponding to the methyl protons of the pentamethylcyclopentadienyl ring.

The mass spectra of all the complexes display the loss of counter ion which is quite common on the case of half sandwich cationic complexes. Complexes (1-3 and 7-9) display their molecular ion peaks at m/z: 635.06, 637.01, 727.10, 544.20, 546.23, and 636.15 respectively which corresponds to the $[\text{M-PF}_6]^+$ ion, whereas complexes (4-6) display their molecular ion peaks at m/z: 634.52, 636.15, and 741.71 which corresponds to the $[\text{M-Cl}]^+$ ion. The peaks

corresponding to the loss of the ligands as well as the arene ring are not observed which indicates the strong metal to ligand and metal to arene bond. The mass spectral values strongly justify the composition and formulation of these complexes.

The UV–visible spectra of complexes (**1-9**) were recorded 20 μ M acetonitrile solution in the range 200-600 nm. All the ligands and complexes showed two bands around 260 and 375 nm. The higher energy band around 245-260 nm is attributed to $n \rightarrow \pi^*$ and $\pi \rightarrow \pi^*$ transitions whereas the lower energy absorption band in the region 350-390 nm are ascribed to metal to ligand charge transfer (MLCT) (Figure S13).

3.3. Single crystal X-ray structure determination of complexes:

The molecular structures of complexes (**1**, **2**, **7** and **8**) were established by single crystal X-ray analysis. Because of low theta value the crystal structures of complexes (**3**, **4** and **6**) are presented here to only confirm the structures and compositions of the molecules. The crystals of the complexes suitable for X-ray diffraction study were obtained by solvent diffusion method by diffusing hexane into a saturated solution of the complexes in dichloromethane. Suitable single crystals were attached to a glass fiber and transferred into the Oxford Diffraction Xcalibur Eos Gemini diffractometer. The ORTEP representations of the complexes at 50% probability along with the crystallographic numbering schemes are depicted in figures (1-3). Crystal data parameters along with selected bond lengths and bond angles are given in the Tables 1 and 2 respectively. Complexes (**1**), (**2**), and (**7**) crystallized in triclinic crystal system with space group PT whereas complex (**8**) crystallized in monoclinic with $P121/n1$ space group. The molecular structures of all these complexes display typical three legged “piano stool” geometry around the metal center which is common for ruthenium, rhodium and iridium half-sandwich compounds [42, 43]. The metal center is coordinated to the *p*-cymene and pentamethylcyclopentadienyl in a

η^6/η^5 manner, which occupies one face of the octahedron, two nitrogen donor atoms from chelating ligand in a bidentate N \cap N fashion and one chloride [44]. The X-ray structure of the complexes reveals the different coordination modes of the ligands to the metal ion. In complexes (**1-3**) the ligand coordinates to the metal center through both the pyridine nitrogen atoms forming a six membered chelate ring whereas in the case of complexes (**4-9**) the ligand coordinates to the metal center through one hydrazone nitrogen and one pyridine nitrogen atom forming a five membered chelate ring as evidenced from the molecular structure.

The metal-centroid bond distances in ruthenium complexes (**1**) and (**7**) { 1.68 Å } are found to shorter than the metal-centroid bond distances in rhodium complexes (**2**) and (**8**) { 1.728 Å } as indicated in Table 2. The Ru–N and Ru–Cl bond distances in complex (**1**) and complex (**7**) are found to be 2.07-2.09 and 2.38-2.39 Å respectively which are consistent with other related system. Likewise, the Rh–N and Rh–Cl bond distances in complex (**2**) and (**8**) are found to be in the range 2.09-2.12 and 2.39- 2.41Å respectively which are also in good agreement with the reported complexes [45]. The bond angle values N1-M-N2 and N-M-Cl in these complexes are very to close 90° which is comparable to the pseudo-octahedral geometry about the metal center.

Furthermore, the crystal structure of complex (**1**) display two different types of intermolecular hydrogen bonding; the first interaction is C-H \cdots O between the nitro - O and H-atom from methyl group of *p*-cymene moiety (2.625 Å), the second C-H \cdots O between the nitro - O and methine hydrogen of *p*-cymene ligand (2.407 Å) (Figure S14). Similarly the crystal structure of complex (**2**) exhibits three different types of intermolecular interactions *viz.* C-H \cdots O (2.674 Å) between the nitro - O and H-atom of pyridyl ring, C-H \cdots Cl (2.616 Å) interaction between chloride atom and aromatic H atom from pyridyl ring and $\pi\cdots\pi$ interaction (4.008Å)

between the two ring of phenylhydrazone group (Figure S15). Complex (7) displays $\pi\cdots\pi$ (4.655 Å) interaction between the two rings of p-cymene moiety as presented in figure S16. The crystal packing of complex (8) exhibit a $\pi\cdots\pi$ (4.175 Å) interaction between two pyridine ring and one C-H $\cdots\pi$ (3.714 Å) interaction of one C-H and one pyridine ring (Figure S17).

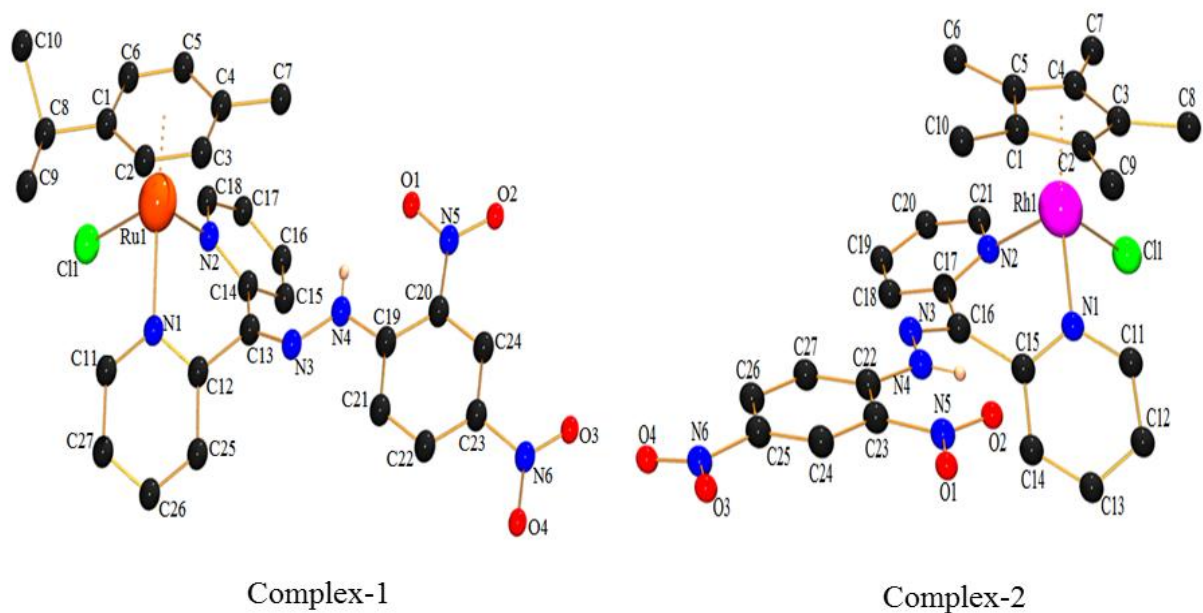


Figure 1. ORTEP rendered views of complex (1) and complex (2) with 50% probability. Hydrogen atoms except N-H and counter ion (PF_6) are omitted for clarity.

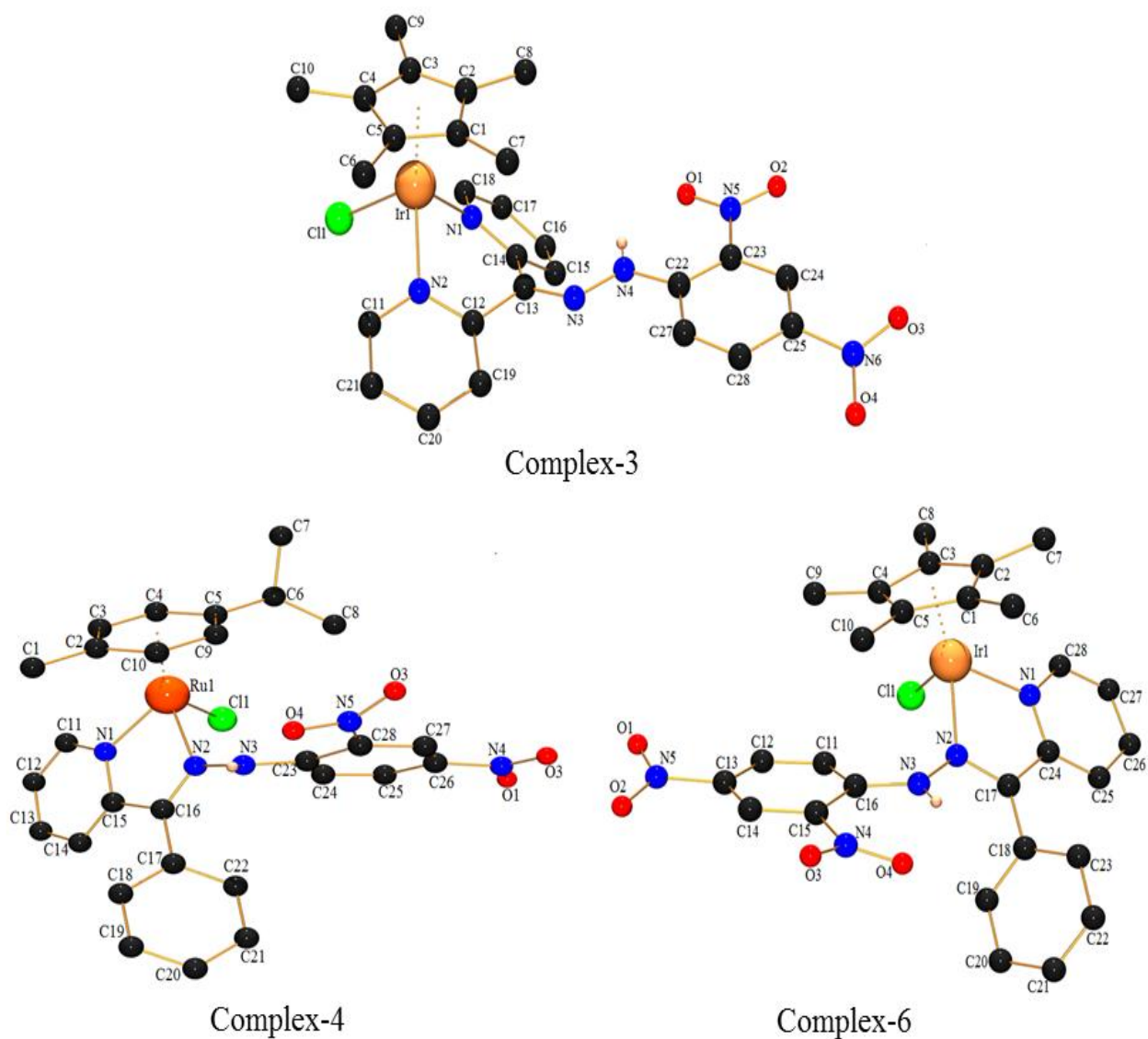


Figure 2. ORTEP rendered views of complex (3), complex (4) and complex (6) with 50% probability. Hydrogen atoms except N-H and counter ion Cl^- are omitted for clarity. Because of low theta value the crystal structure of these complexes are presented here to only confirm the structure and composition of molecule.

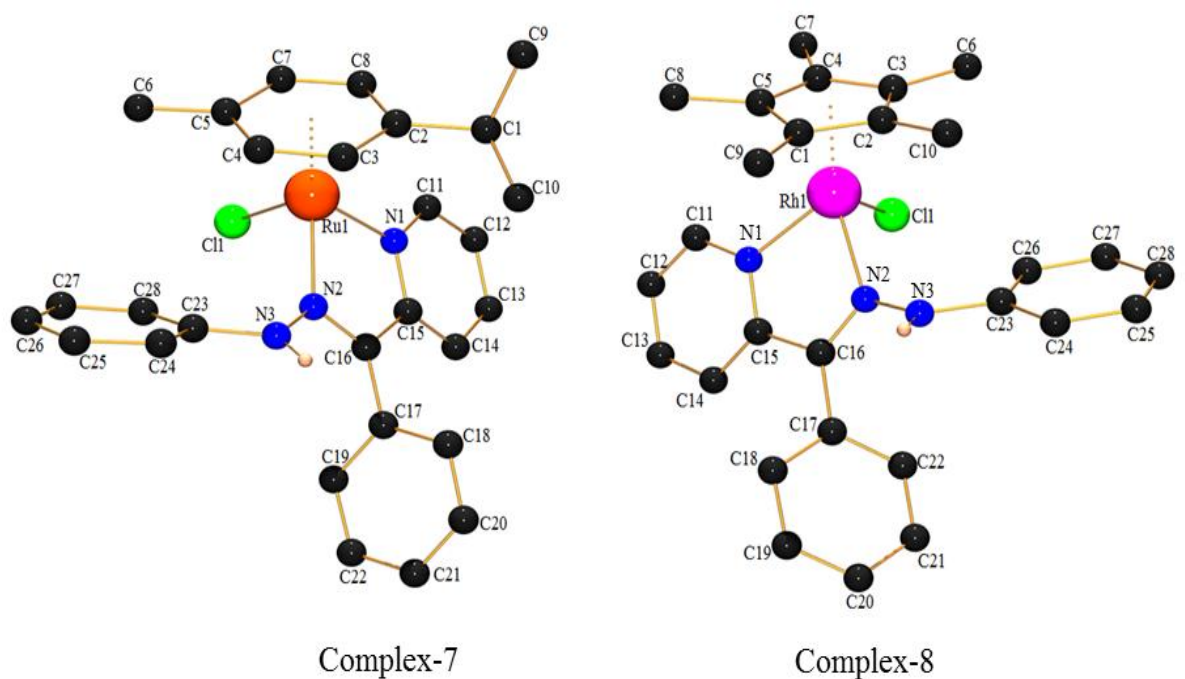


Figure 3. ORTEP rendered views of complex (7) and complex (8) with 50% probability. Hydrogen atoms except N-H and counter ion (PF_6) are omitted for clarity.

3.4. *In vitro* antimicrobial assay

The starting metal precursor complexes, synthesized ligands and complexes were tested for their activity against two Gram positive bacteria *S. aureus* and *B. thuringiensis* and two Gram negative bacteria such as *E. coli* and *P. aeruginosa* taking gentamycin as a positive control. The starting precursor of $[(p\text{-cymene})\text{RuCl}_2]_2$ were found to be inactive as reported in the previous literature [46]. We have carried out the antimicrobial activity of $[\text{Cp}^*\text{RhCl}_2]_2$ and $[\text{Cp}^*\text{IrCl}_2]_2$ but none of them show any significant activity. This indicates that the antimicrobial activity is solely attributed to the ligands and the metal-ligand complexes. The effectiveness of an antibacterial agent in sensitivity testing is based on the size of the diameter of zones of inhibition against the tested organism. The histograms of the resultant zone of inhibition are presented in Figure 4 and Figure 5. The diameter of the zone is measured to the nearest millimeter, and the results are

summarized in Table 3. For Gram negative bacteria, it was found that all the complexes show maximum antibacterial selectivity against *P. aeruginosa*. However, none of the complexes show significant antimicrobial activity against *E.coli* bacteria.

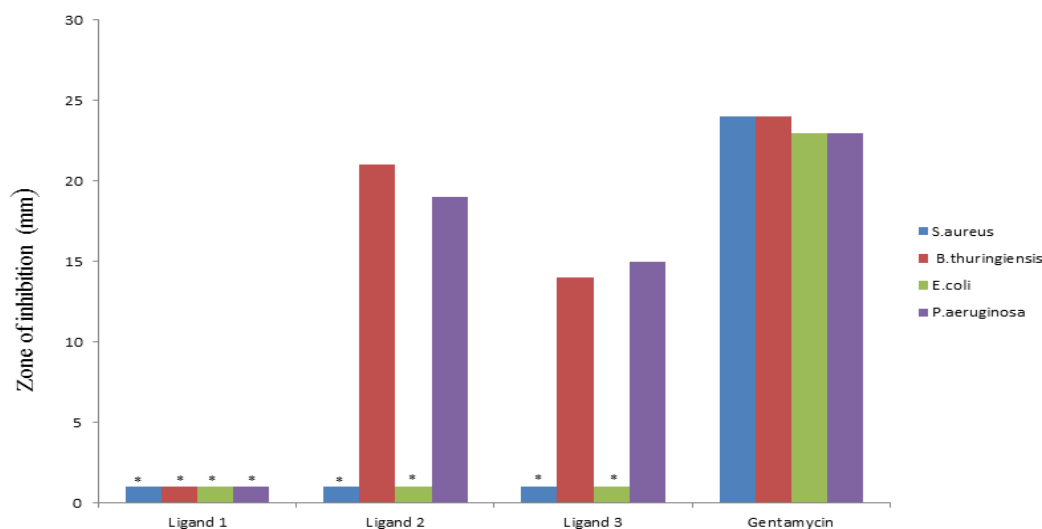


Figure 4. Histogram of the zone of inhibition (mm) of the ligands (1-3) in comparison with gentamycin. Where “*” indicates that compound exhibited no zone of inhibition. All the complexes expressed standard deviation of error with in the ± 2 and ± 1 .

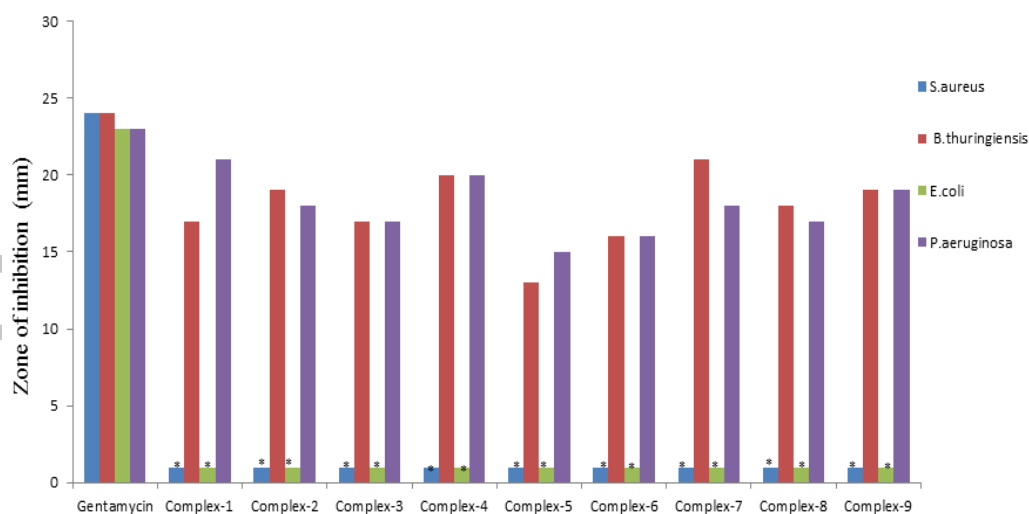


Figure 5. Histogram of the zone of inhibition (mm) of the complexes (**1-9**) in comparison with gentamycin. Where “*” indicates that compound exhibited no zone of inhibition. All the complexes expressed standard deviation of error with in the ± 2 and ± 1 .

Similarly, in the case of Gram positive bacteria it was found that all the complexes show antibacterial selectivity against *B. thuringiensis* with significant activity. However, these complexes did not show any noticeable activity for *S.aureus*. Among the ligands, **L2** are more effective in inhibiting the specific bacteria, **L3** showed moderate activity whereas **L1** did not show any activity for all the selected bacteria. As evident from the results all *p*-cymene ruthenium complexes showed good activity against *P. aeruginosa* and *B. thuringiensis* compared to Cp*Rh and Cp*Ir complexes. However, complexes have not superseded the activity of the standard gentamycin. These observations indicate that all the complexes are exclusive to particular strains of both gram-positive and gram negative bacteria evidencing them as strong selective antibacterial agents.

DNA binding studies of platinum group metal complexes

The biological activity of platinum group metal complexes such as half-sandwich ruthenium, rhodium and iridium metal complexes has been partially attributed to their interaction with DNA molecules [47]. In order to elucidate any such kind of interaction is present between the newly synthesized complexes with DNA; we have performed titration experiments with fluorescent metal complexes (Ligand **1**, Complex **1** and complex **2**) using SM-DNA as a biomolecule. The emission spectra of these complexes on increasing amounts of SM-DNA do not show a significant change in the spectral intensity or peak shift even up to a ratio of 1:2 (Figure. S18). Hence, these titration experiments clearly evidenced that none of the chosen platinum group metal complexes containing phenyl hydrazone Schiff base ligands does not bind

to DNA, which is in contrast to Cisplatin and other known platinum group complexes that form DNA adducts [48].

4. Conclusion

In summary, we have successfully synthesized a series of nine mononuclear complexes of *p*-cymene ruthenium, Cp* rhodium and Cp* iridium with phenyl hydrazone derived ligands **L1**, **L2** and **L3**. The complexes were obtained in good yields. All the complexes were characterized by various spectroscopic studies and X-ray analysis. Spectral studies strongly support the formation of the compounds. The X-ray structure of the complexes reveals the different coordination modes of the ligands to the metal ion. In complexes (**1-3**) the ligand coordinates to the metal center through both the pyridine nitrogen atoms forming a six membered chelate ring whereas in the case of complexes (**4-9**) the ligand coordinates to the metal center through one hydrazone nitrogen and one pyridine nitrogen atom forming a five membered chelate ring as evidenced from the molecular structure. All the nine complexes investigated in the present study exhibited interesting selectivity in the antibacterial studies performed against four pathogenic bacteria viz., *S. aureus*, *E. coli*, *B. thuringiensis* and *P. aeruginosa* with zone of inhibition in the range of 13–21 mm. All the complexes exhibit selectivity for *P. aeruginosa* and *B. thuringiensis* by showing better activity and it did not show any activity against the bacteria *E.coli* and *S.aureus*.

Acknowledgements

Agreeda Lapasam thanks UGC, New Delhi, India for providing financial assistance in the form of university fellowship (UGC-Non-Net). I thank DST-PURSE SCXRD, NEHU-SAIF, Shillong, India for providing Single crystal X-ray analysis and other spectral studies.

Appendix A. Supplementary data

CCDC **1842504** (1), **1842505** (2), **1842506** (7) and **1842507** (8) contains the supplementary crystallographic data for this paper. These data can be obtained free of charge via www.ccdc.cam.ac.uk/data_request/cif, by e-mailing data_request@ccdc.cam.ac.uk, or by contacting The Cambridge Crystallographic Data Centre, 12, Union Road, Cambridge CB2 1EZ, UK; Fax: +44 1223 336033.

Reference

- [1] C. Fred, *The American Journal of Med.* 119 (2006) S3.
- [2] M. Rookaya, L.M. Karenchak, E.G. Romanowki, R.P. Kowalski, *American Journal of ophthal.* 133 (2002) 463.
- [3] M. Krishnamoorthy, S. Hakobyan, M. Ramstedt, J. E. Gautrot, *Chem. Rev.* 114 (2014) 10976.
- [4] H. Zhang, H.B. Liu, J.M. Yue, *Chem. Rev.* 114 (2014) 883.
- [5] J. Li, G. Wang, H. Zhu, M. Zhang, X. Zheng, Z. Di, X. Liu, X. Wang, *Sci. Rep.*, 4 (2014) 4359.
- [6] R. Liu, X. Chen, S. Chakraborty, J.J. Lemke, Z. Hayouka, C. Chow, R.A. Welch, B. Weisblum, K.S. Masters, S.H. Gellman, *J. Am. Chem. Soc.* 136 (2014) 4410.
- [7] C. Fasciani, M.J. Silvero, M.A. Anghel, G.A. Arguello, M.C. Becerra, J.C. Scaiano, *J. Am. Chem. Soc.*, 136 (2014) 17394.
- [8] S. Dodbele, C. D. Martinez, J.M. Troutman, *Biochemistry* 53 (2014) 5042.
- [9] S.B. Levy, B. Marshall, *Nat. Med.* 10 (2004) 122.
- [10] M. Martinez, P.N. Silley, *Engl. J. Med.* 335 (2010) 1445.

- [11] D.J. Payne, M.N. Gwynn, D.J. Holmes, D.L.N. Pompliano, *Engl. J. Med.* 6 (2007) 29.
- [12] A. Sonia, D. Harvell, E. Friedle, *Trends in Ecology & Evolution*, 18 (2003) 589.
- [13] C. Loncle, J.M. Brunel, N. Vidal, M. Dherbomez, Y. Letourneux, *Eur. J. Med. Chem.* 39(2004) 1067.
- [14] Y. Xia, C. Fan, B. Zhao, J. Zhao, D. Shin, J. Miao, *Eur. J. Med. Chem.* 43 (2008) 2347.
- [15] G.U. Salgin, K. N. Gokham, O. Gostal, Y. Koysal, E. Kilici, S. Isik, G. Aktay and M. Ozalp, *Bioorganic & Medicinal Chemistry*, 15, No. 17 (2007) 5738.
- [16] P. Melnyk, V. Leroux, C. Sergheraert, P. Grellier, *Design, Bioorg. Med. Chem. Lett.* 16 (2006) 31.
- [17] M.T. Cocco, C. Congiu, V. Lilliu, V. Onnis, *Bioorg. Med. Chem.* 14 (2006) 366.
- [18] S. Lörinc, J. Švorec, M. Melník, M. Koman, *Polyhedron*, 27 (2008) 3545.
- [19] D.K. Demertzi, M. Staninska, I.G. Santos, A. Castineiras, M.A. Demertzis, *J. Inorg. Biochem.* 105 (2011) 1187.
- [20] Y.H. Zhou, W.Q. Wan, D.L. Sun, J. Tao, L. Zhang, X.W. Wei, *Anorg. Allg. Chem.* 640 (2014) 249.
- [21] D. Sun, Y. Liu, D. Liu, R. Zhang, X. Yang, J. Liu, *Chem. Eur. J.* 18 (2012) 4285.
- [22] C.S. Allardyce, P.J. Dyson, *Platinum Met. Rev.* 45 (2001) 62.
- [23] B. Nordén, P. Lincoln, B. Akerman and E. Tuite, *Met. Ions Biol. Syst.*, 33 (1996) 177.
- [24] N.W. Luedtke, J. S. Hwang, E. Nava, D. Gut, M. Kol and Y. Tor, *Nucleic Acids Res.* 31 (2003) 5732.
- [25] C. Metcalfe, J.A. Thomas, *Chem. Soc. Rev.* 32 (2003) 215.
- [26] B.M. Zeglis, V.C. Pierre and J.K. Barton, *Chem. Commun.* (2007) 4565.

- [27] F.R. Keene, J.A. Smith and J.G. Collins, *Coord. Chem. Rev.* 253 (2009) 2021.
- [28] M.R. Gill, J.A. Thomas, *Chem. Soc. Rev.* 41 (2012) 3179.
- [29] F.P. Dwyer, D.P. Mellor, *Chelating Agents and Metal Chelates*, Academic Press, New York, 1964.
- [30] C.A. Puckett and J.K. Barton, *Biochemistry*, 47 (2008) 11711.
- [31] M.R. Gill, J. Garcia-Lara, S.J. Foster, C. Smythe, G. Battaglia and J.A. Thomas, *Nat. Chem.*, 1, (2009) 662.
- [32] M. Matson, F.R. Svensson, B. Nordén and P. Lincoln, *J. Phys. Chem. B*, 115 (2011) 1706.
- [33] [a] Y. Geldmacher, M. Oleszak, W.S. Sheldrick, *Inorg. Chim. Acta* 393 (2012) 84.
(b) M.A. Scharwitz, I. Ott, Y. Geldmacher, R. Gust, W. Sheldrick, *J. Organomet. Chem.* 693 (2008) 2299.
(c) M. Gras, B. Therrien, G. Suss-Fink, A. Casini, F. Edafe, P.J. Dyson, *J. Organomet. Chem.* 695 (2010) 1119.
(d) J. Canivet, G. Suss-Fink, P. Stepnicka, *Eur. J. Inorg. Chem.* 2007, 4736.
(e) Z. Lui, P.J. Sadler, *Acc. Chem. Res.* 47 (2014) 1174.
(f) A. B. Punna Rao, M. Kalidasan, K. Gangel, D.K. Deb, S.L. Shepherd, R.M. Phillips, K.M. Poluri, K.M. Rao, *Chem. Select*, 2 (2017) 2065-2076.
(g) A.B. Punna Rao, A. Uma, T. Chiranjeevi, M.S. Bethu, B. Yashwanth, J.V. Rao, K.M. Poluri, K.M. Rao, *Inorg. Chim. Acta*, 453 (2016) 284–291.
- [34] A. Bolhuis, L. Hand, J.E. Marshall, A.D. Richards, A. Rodger and J. Aldrich-Wright, *Eur. J. Pharm. Sci.* 42 (2011) 313.
- [35] M.A. Bennett, T.N. Huang, T.W. Matheson, A.K. Smith, S. Ittel, W. Nickerson,

- Inorg. Synth., 21 (1982) 74.
- [36] C. White, A. Yates, P.M. Maitlis, D.M. Heinekey, Inorg. Synth., 29 (2007) 228.
- [37] G.M. Sheldrick, Acta Crystallogr. Sect.A, 46 (1990) 467.
- [38] G.M. Sheldrick, Acta Crystallogr. Sect.A, 64 (2008) 112.
- [39] L.J. Farrugia, J. Appl. Crystallogr., 32 (1999) 837.
- [40] V.K. Gupta, A.K. Singh, S Bhardwaj, K. Rao Bandi, Sensors and Actuators B 197 (2014) 264.
- [41] A.R. Despaigne, J.G. Da Silva, A.M. do Carmo, Oscar E. Piro, E.E. Castellano, H Beraldo, Inorg. Chim. Acta 362 (2009) 2117.
- [42] K.S. Singh, P.J Carroll, K.M. Rao, Polyhedron 24 (2005) 391.
- [43] P. Govindaswamy, J. Canivet, G. Suss-Fink, P. Stepnicka, J Ludvik , K.M. Rao, J. Organomet. Chem 692 (2007) 3664.
- [44] T. Tsolis, M.J. Manos, S. Karkabounas, I. Zelovitis, A. Garoufis, J. Organomet. Chem. 768 (2014) 1.
- [45] S. Sangilipandi, R. Nagarajaprakash, D. Sutradhar, W. Kaminsky, A.K. Chandra, K. Mohan Rao, Inorg. Chim. Acta 437 (2015) 177.
- [46] C.S. Allardyce, P.J. Dyson, D.J. Ellis, P.A. Salter, R. Scopelliti, J. Organomet. Chem. 668 (2003) 35-42.
- [47] Andre F. LeRoy, Environmental Health Perspectives 10 (1975) 73.
- [48] Adnan Salim, Abu Surrah, Mika Kettunen, Curr. Med. Chem., 13 (2006) 1337.

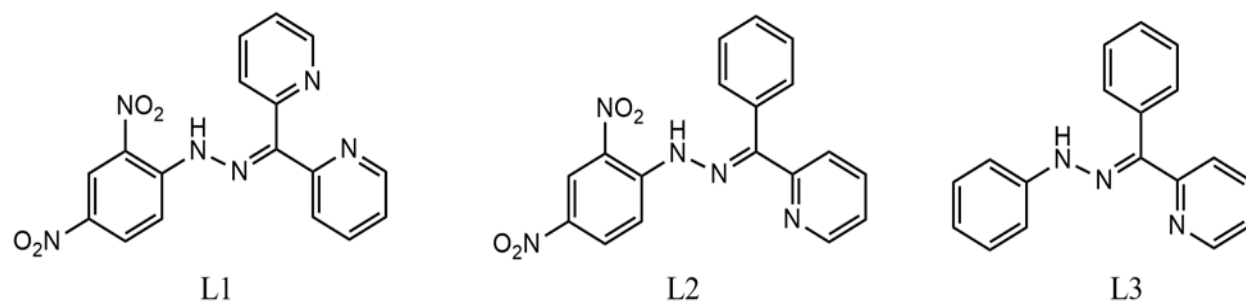
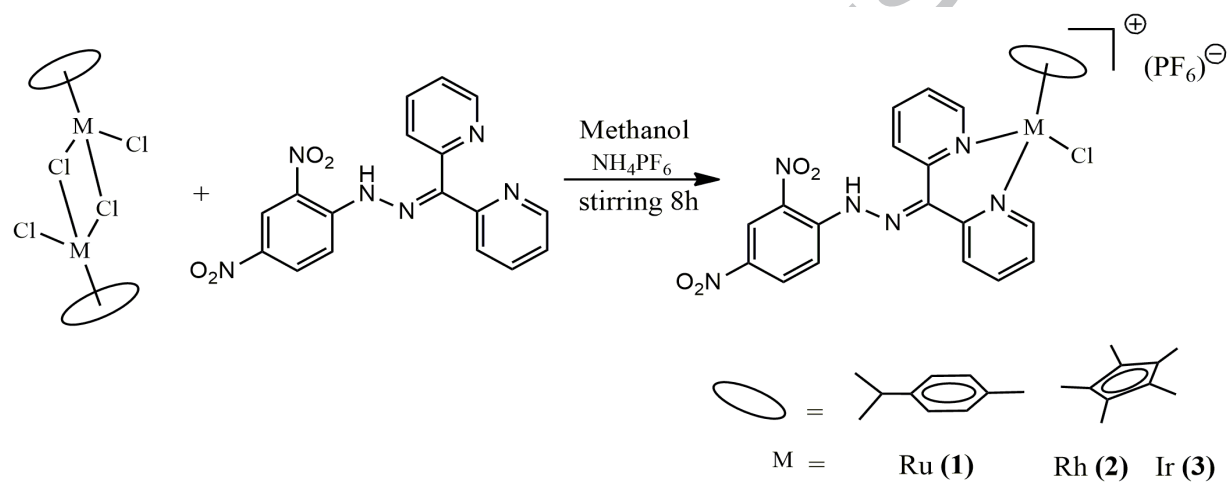
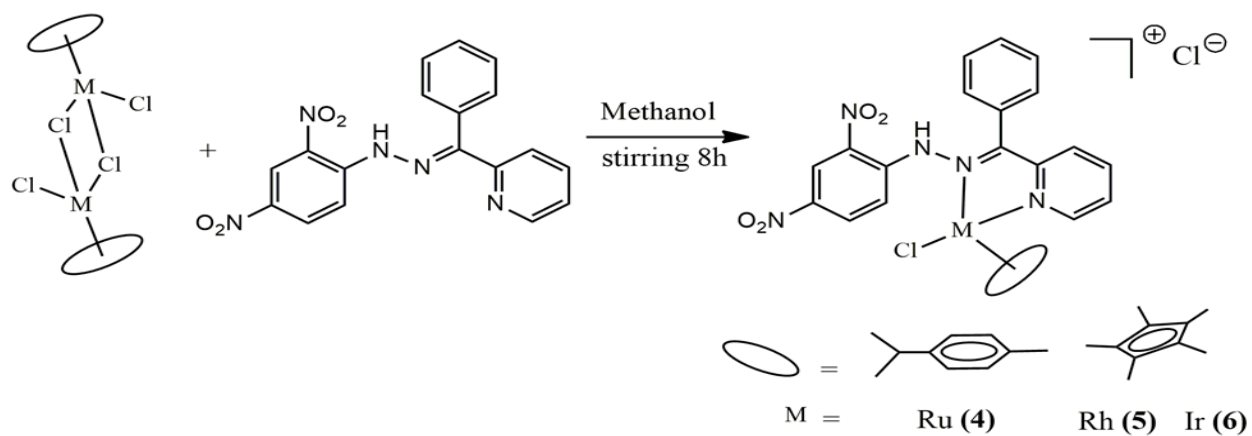


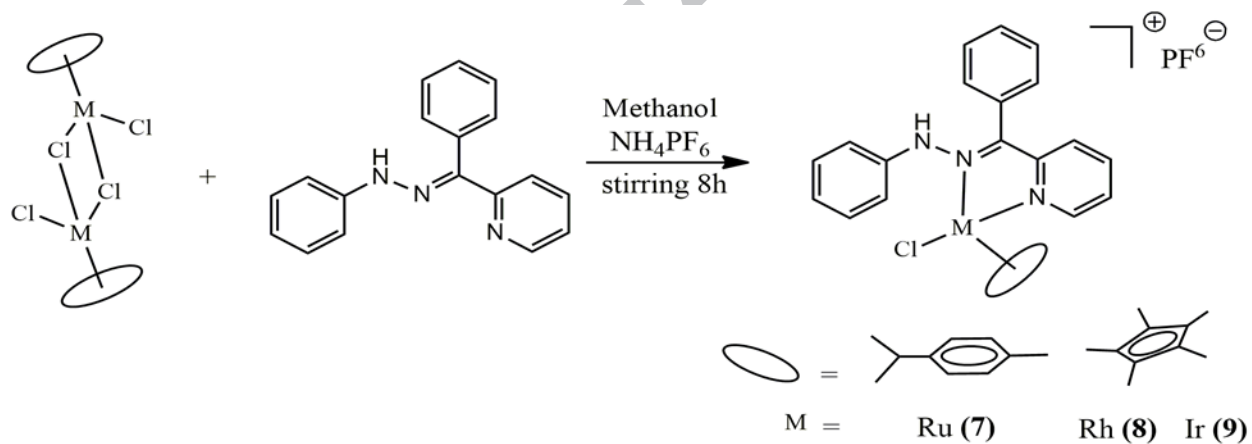
Chart 1: Ligands used in the present study



Scheme 1: Schematic representation of the synthesis of complexes (**1-3**).



Scheme 2: Schematic representation of the synthesis of complexes (4-6).



Scheme 3: Schematic representation of the synthesis of complexes (7-9).

Table 1. Crystal data and structure refinement details of complexes.

Complexes	1	2	7	8
Empirical formula	C ₂₇ H ₂₆ ClN ₆ O ₄ RuPF ₆	C ₂₇ H ₂₇ ClF ₆ N ₆ O ₄ PRh	C ₂₈ H ₂₉ ClN ₃ RuPF ₆	C ₂₈ H ₃₀ ClN ₃ RhPF ₆
Formula weight	780.03	782.87	689.03	691.88
Temperature (K)	293 (2)	293(2)	293.0 (2)	293.0 (2)
Wavelength (Å)	0.71073	0.71073	0.71073	0.71073
Crystal system	Triclinic	Triclinic	Triclinic	'monoclinic'
Space group	' <i>P</i> <i>T</i> '	' <i>P</i> <i>T</i> '	' <i>P</i> <i>T</i> '	' <i>P</i> 121/ <i>n</i> 1'
a (Å)/α (°)	8.2067(3)/84.430(4)	8.9243(5)/92.281(3)	10.4195(5)/104.857(5)	11.3169(6)/90
b (Å)/β (°)	13.1749(6)/87.712(3)	12.6858(5)/107.099(4)	10.8269(5)/94.486(5)	8.6057(5)/96.606(4)
c (Å)/γ (°)	14.4250(7)/80.885(3)	14.7599(6)/97.993(4)	14.1435(10)/102.316(4)	30.0275(15)/90
Volume (Å ³)	1532.22(12)	1575.86(13)	1491.71(15)	2905.0(3)
Z	2	2	1	4
Density (calc) (Mg/m ³)	1.691	1.650	1.534	1.582
Absorption coefficient (μ) (mm ⁻¹)	0.732	0.757	0.729	0.797
F(000)	784	788	696	1400
Crystal size (mm ³)	0.25 x 0.21 x 0.19	0.23 x 0.18 x 0.15	0.39 x 0.25 x 0.23	0.25 x 0.16 x 0.12
Theta range for data collection	3.7890 to 25.0470	4.1600 to 26.3690	4.0220 to 26.1770	3.8840 to 27.0480
Index ranges	-10<=h<=10, -17<=k<=12, -19<=l<=17	-10<=h<=11, -13<=k<=17, -20<=l<=20	-11<=h<=13, -14<=k<=14, -19<=l<=12	-14<=h<=15, -10<=k<=11, -40<=l<=18
Reflections collected	10665	11090	10287	12195
Independent reflections	6879 [R(int)=0.0393]	7137 [R(int)=0.0376]	4789 [R(int)=0.0340]	5318 [R(int)=0.0347]
Completeness to theta = 25.00°	99.15	99.41	99.36	99.04
Absorption correction	Semi-empirical from equivalents	Semi-empirical from equivalents	Semi-empirical from equivalents	Semi-empirical from equivalents
Refinement method	Full-matrix least-squares on F ²	Full-matrix least-squares on F ²	Full-matrix least-squares on F ²	Full-matrix least-squares on F ²
Data/restraints/parameters	6879/0/415	7137/0/415	6711/0/361	6617/0/361
Goodness-of-fit on F ²	1.056	1.036	1.023	1.116
Final R indices [I>2σ(I)]	R1 = 0.0617, wR2 = 0.1265	R1 = 0.0598, wR2 = 0.1408	R1=0.0629, wR2= 0.1566	R1=0.0651, wR2 = 0.1351
R indices (all data)	R1 = 0.0873, wR2 = 0.1406	R1 = 0.0865, wR2 = 0.1591	R1=0.0895, wR2=0.1786	R1=0.0864, wR2 = 0.1460
Largest diff. peak and hole (e.Å ⁻³)	0.713 and -0.458	0.924 and -0.747	0.983 and -0.704	0.678 and -0.695
CCDC No.	1842504	1842505	1842506	1842507

Structures were refined on F_0^2 : $wR_2 = [\sum[w(F_0^2 - F_c^2)^2] / \sum w(F_0^2)^2]^{1/2}$, where $w^{-1} =$

$$[\sum(F_0^2) + (aP)^2 + bP] \text{ and } P = [\max(F_0^2, 0) + 2F_c^2]/3$$

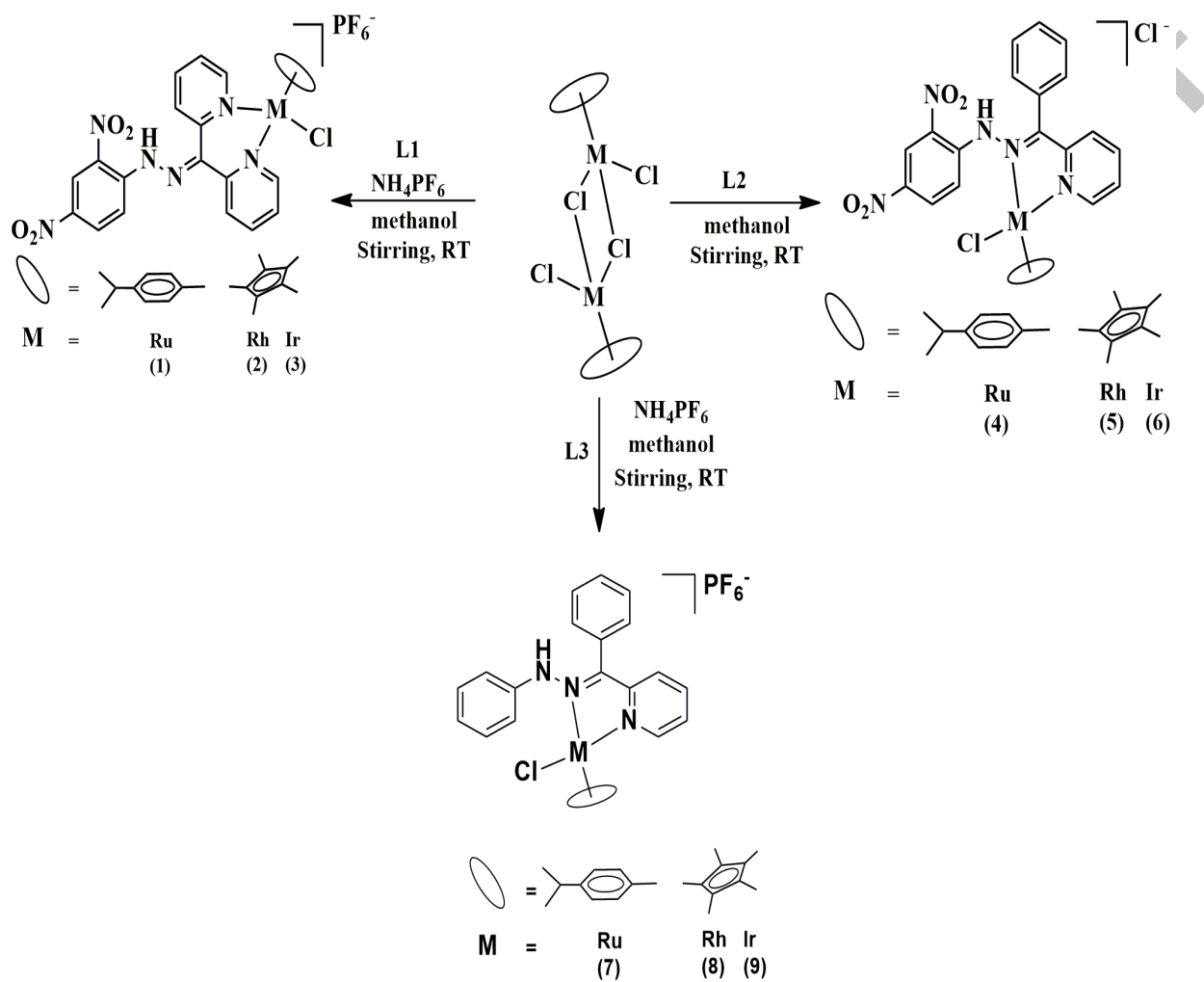
Table 2: Selected bond lengths (Å) and bond angles (°) of complexes

Complexes	1	2		7	8
Bond distances (Å)			Bond distances (Å)		
M(1)-CNT	1.689	1.784	M(1)-CNT	1.686	1.787
M(1)-N(1)	2.099(4)	2.096(3)	M(1)-N(1)	2.074(4)	2.097(4)
M(1)-N(2)	2.093(4)	2.119(4)	M(1)-N(2)	2.098(3)	2.120(4)
M(1)-Cl(1)	2.394(1)	2.399(1)	M(1)-Cl(1)	2.384(2)	2.412(1)
N(3)-N(4)	1.344(6)	1.344(7)	N(2)-N(3)	1.367(5)	1.390(6)
Bond Angles (°)			Bond Angles (°)		
N(1)-M(1)-N(2)	84.8(2)	86.2(1)	N(1)-M(1)-N(2)	76.3(2)	76.0(1)
N(1)-M(1)-Cl(1)	85.9(1)	87.6(1)	N(1)-M(1)-Cl(1)	82.4(1)	83.3(1)
N(2)-M(1)-Cl(1)	86.9(1)	87.1(1)	N(2)-M(1)-Cl(1)	91.6(1)	91.4(1)

Table 3: Resultant zone of inhibition

Sl. No.	Compounds	Bacterial Strains			
		Gram negative		Gram positive	
		E.coli	P. aeruginosa	S.aureus	B. thuringiensis
+ve control	Gentamycin	23±2	23±2	24±2	24±2
1	Ligand 1	-	-	-	-
2	Ligand 2	-	19±2	-	21±1
3	Ligand 3	-	15±1	-	14±2
4	Complex 1	-	21±2	-	17±1
5	Complex 2	-	18±2	-	19±2
6	Complex 3	-	17±1	-	17±2
7	Complex 4	-	20±2	-	20±1
8	Complex 5	-	15±1	-	13±1
9	Complex 6	-	16±2	-	16±1
10	Complex 7	-	18±2	-	21±2
11	Complex 8	-	17±1	-	18±1
12	Complex 9	-	19±1	-	19±1

Graphical abstract



HIGHLIGHTS

1. Mononuclear phenylhydrazone complexes of Ru, Rh and Ir have been isolated.
2. Metal complexes have shown good activity against *P. aeruginosa* and *B. thuringiensis*

ACCEPTED MANUSCRIPT